

Transformation of Type I Fuzzy Logic into Interval Type II Fuzzy Logic-based Unit Voltage Template with Controlled Load

Muhannad Drak Alsebai^{1*}, Kishore Kumar Pedapenki¹

¹ Department of Electrical and Electronics Engineering, Jain (Deemed-To-Be University), 45th km, NH - 209, Jakkasandra Post, Bengaluru-Kanakapura Main Road, 562112 Bengaluru, Karnataka, India

* Corresponding author, e-mail: muhannad.drak@jainuniversity.ac.in

Received: 24 April 2023, Accepted: 06 September 2023, Published online: 31 October 2023

Abstract

The interval type II fuzzy logic controller (IT2FL) is a recent artificial intelligent technology which is applied in many aspects of electrical power engineering and controlling strategies these days. The improving of Distribution Static Synchronous Compensator (DSTATCOM) control algorithms is still ongoing, because the control strategy of DSTATCOM device is considered as a decisive factor which affects the performance of DSTATCOM device in enhancing the quality of power in the distribution grids. The improving process focuses in two main aspects the DC capacitor voltage response to the control system and the mitigation of the harmonics which are produced by the controlled and uncontrolled rectified loads. In this paper, the interval type II fuzzy logic controller (IT2FL) based the Unit Voltage Template strategy (UVT) is examined by the MATLAB program with two different ranges of input signals, and compared with the type I Fuzzy logic controller (T1FL). The IT2FL based UVT shows promising results in improving the deformed shape of source current waves in comparison with the other controllers.

Keywords

DSTATCOM, device, unit voltage template control algorithm, interval type II fuzzy logic controller, type I fuzzy logic controller

1 Introduction

The power quality term is widespread these days in the distribution electrical grids, which means the ability of the source to supply the load with current and voltage waves which are pure harmonics-free without deformation [1, 2]. It becomes one of the customers and producers' important priority these days. The customers of the electrical system nowadays are utilizing variety load types causing the deformation of electrical source current waves and drive them away from a sinusoidal, which affects the power quality negatively and increases the necessity of the improvement process [3]. In some nonlinear loads such as Diode Bridge Rectifier (DBR) with Brushless DC Motor (BLDC motor), the total harmonic distortion of source current reaches to 70% and the source power factor becomes under 0.7, and these values are not acceptable by the international power quality standards [4–6]. Furthermore, Induction motor, which uses DBR and Space Vector Modulation (SVM) inverter to control its speed, produces noise and disturbances to the power system [7]. Power quality disturbances can be identified as any deviation may happen in the sinusoidal shape in the voltage

or current waveforms [8]. The smart grids suffer from the power quality disturbances more than the traditional grids, because of the high penetration of the renewable energy sources in the smart grids in comparison with the traditional one [9, 10]. The electrical disturbances can be classified as harmonics, unbalanced load, flickers, voltage swell and voltage sag. They may cause an excessive heat for the electrical appliances and increasing of the power losses in the transmission and distribution grids [11].

For the improvement process, inverter-based power quality conditioners are used in these days, because of their small size and fast response in comparison with conventional ways [12–14]. The utilizing of Distribution Static Synchronous Compensator (DSTATCOM) device in the distribution grid compensates the reactive power, returns the electrical current waves to sinusoidal form, leading to the enhancement the power quality [15–17].

The multilevel inverters are used recently for the medium and high-power loads because of their ability to produce a high voltage without using transformers. The high voltage can be obtained by using many levels of

small voltage to reach the desired high voltage. These multilevel inverters can be achieved by utilizing additional switching devices which need complicated control strategy to provide them with the necessary pulses [18–20].

DSTATCOM device is one of the Shunt Distributed Flexible AC Transmission System (DFACTS) devices, which is connected in parallel with the distribution grid. The working principle of DSTATCOM device is to inject the compensating current into the distribution grid to reduce harmonics, compensate the reactive power, maintain power factor, balance the load [21].

The performance of DSTATCOM device in improving the power quality depends on the effectiveness of control strategy and the controller used. Many conventional control strategies have been used to improve the performance of DSTATCOM device. Besides, the control strategies should have features of fast response and load change tracking to meet the requirements of controlling and operating smart grids [22–24]. Unit voltage template control depends on the principle of unites the phases of the current and voltage source waves to improve the power factor [25, 26]. Many controllers were an applied to these control strategies, such as: PI controller, neural network and type I fuzzy logic [27–29]. PI controller is considered as linear controller which needs the linear model of the controlled system, while the artificial neural network and fuzzy logic controller are considered as linear and non-linear controllers which doesn't need the nonlinear model of the controlled system [30–32]. Consequently, the use of artificial intelligence controllers is recommended when the model of the controlled system can't be reached easily [33].

The best performance of DSTATCOM device can be achieved with PI controller with the suitable selection of the proportional and integral gains for a specific condition of the load [34].

The application of IT2FL with the UVT control algorithm is not implemented, even though, that UVT control algorithm give fast response and better harmonics mitigation in comparison with the other control strategies, because it does not need to utilize Low Pass filter (LPF) for filtering the input signals in comparison with the other control algorithms.

In this paper, the utilizing of IT2FL controller with UVT is implemented to control the DC Capacitor voltage of the DSTATCOM device instead of PI, to improve the DSTATCOM device performance in the mitigation of the source current harmonics, and to improve the DC capacitor response of the DSTATCOM device.

First, the tuning process of T1FL and IT2FL controllers based UVT control strategy takes place in the response to different controlled rectified load situations with two different ranges of input signals. Second, The T1FL and IT2FL controllers based UVT control strategy is examined by using MATLAB environment with two different ranges of input signals at different load situations. Third, The T1FL and IT2FL controllers based UVT control strategy is examined by using MATLAB environment at different loads and disturbances in one wave form situation. Fourth, the comparison between two different ranges of input signals was conducted, to define the better controller based UVT in improving the shape of source current waves and keep them with the same phase of the source voltage waves. Two aspects were used to examine the new intelligent IT2FL based UVT; the DC capacitor response parameters as settling, peak and rising time; the electrical source parameters as source power factor and Source current-THD.

2 Review of literature

The type I fuzzy logic has been utilized in many papers to control DSTATCOM device in the past [35]. First, a combination of the fuzzy logic controller along with PI controller were utilized to merge the benefits of both controllers in one strategy. First loop was used to keep the DC capacitor constant, while the second loop were used to extract the reference source currents [36]. Second, the type I fuzzy logic were used as an adjuster to tune the PI controller in the double-loop control strategy [37]. Third, the fuzzy logic controller used to change the proportional and integration gains in the respect of the load changing instantaneously. A new strategy of varying the PI gains to suit the transient situation has been utilized [38]. Fourth, new inputs for fuzzy logic controller used as a trial for improvement. This control strategy used the speed variation and acceleration of the generator as inputs for the fuzzy logic controller and it compared with the PI controller [39]. Fifth, A combination between two fuzzy logic controllers is used to generate the reference source current. The two fuzzy logic controllers are used to control the direct and quadrature axis of the load current wave. The error and change of error of direct and quadrature components of the load current are used as inputs for the two fuzzy logic controllers used in [16]. Sixth, Fuzzy logic controller was used alone for controlling the active power filter. The fuzzy logic controller is applied to the active power filter to diminish the harmonics in the supply side feeding three phase induction motor by utilizing vertical speed indicator (VSI), and it compared with PI and PID

controllers [40]. A fuzzy logic controller was applied to control the active power filter and compared with neuro-fuzzy logic controller [41]. After the application of the type I fuzzy logic the researcher started to face the uncertainty problem which is considered as one of type I fuzzy logic drawbacks [37].

IT2FL controller is one of the artificial intelligence controllers which can overcome the uncertainty situation which the T1FL controller can't handle. IT2FL controller can be tuned easily to handle the nonlinear situations because it has strong learning ability and the ability to be adaptive with system parameters changing [42, 43]. First, IT2FL controller was applied alone with control strategy to control the DSTATCOM device. The IT2FL with SRF control strategy was utilized for improving the source power quality for hospital load which is considered as sensitive loads. The authors compared the interval type II fuzzy logic controller based recursive least square filter with PI and type I fuzzy logic controllers to show the improvement of control strategy [44]. The IT2FL with seven membership functions was utilized to control shunt-high-voltage DSTATCOM device to make suitable for all types of loads which connected either to low voltage busbar or high voltage bus bar [45]. Second, IT2FL was utilized to change proportional and integral gains of the PI controller. The output of IT2FL was used along with the direct component of load current to tune the proportional and integral gains of the PI controller, to give the best mitigation to the source current harmonics and best DC capacitor response parameters. A new structure of interface bank inductor also used to enhance the performance of DSTATCOM device [46]. Third, IT2FL controller was utilized to control a DSTATCOM with complicated structures which is hard to be controlled by PI or T1FL controllers. IT2FL is utilized in the instantaneous reactive power strategy to generate the reference current signals. This control strategy is used to control the three-level active neutral point clamped DSTATCOM device with special structure [42]. Interval type II fuzzy logic was utilized with least mean square control strategy to control the five-level cascade H-Bridge Multi Level Inverter (CHBMLI) DSTATCOM device and compare it with the PI controller [43].

Artificial Neural network (ANN) is considered as one of artificial intelligence controllers which can be utilized with complicated PQ problems that may face the DSATCOM device, because it offers fast dynamic response, better steady state and transient stability to the control system. The common types of ANN which utilized

to control the DSTATCOM device are backpropagation (BP) and ADALINE. Five ANN controllers were trained and used to replace PI controller and all the LPFs in the IRP theory algorithm to improve the DSTATCOM device in the mitigation of the harmonics [47–49].

3 DSTATCOM device

In this paper, three-phase four-wire DSTATCOM device is used for the mitigation of source current harmonics and to unite the phases of voltage and current source waves, while the application controlled rectified loads with resistance and inductor connected in series ($R = 16 \Omega$, $L = 16 \text{ mH}$, $R = 20 \Omega$, $L = 20 \text{ mH}$, $R = 24 \Omega$, $L = 24 \text{ mH}$). The voltage source inverter (VSI) is used to inject or absorb the reactive power needed from the energy stored in the DC capacitor and through three interface inductors to the examined electrical grid. The characters of DSTATCOM device for different controlled rectified loads is listed in the Table 1 [50].

4 Control algorithms

4.1 Unit voltage template theory control algorithm

This control algorithm extracts the reference source current waves, and then compare them with the sensed source current to generate the error signals. These error signals are the inputs for the hysteresis controller which extracts six pulses for the six thyristors of the DSTATCOM device three phases, and extracts two pulses for the two thyristors of the DSTATCOM device neutral.

The desired reference source current waves should have the same phase of the source voltage waves. In order to extract the desired reference source currents, the phases of the source voltage waves are needed to be extracted by the means of the Eqs. (1)–(3) as follows [25]:

$$V_{a.pu} = \frac{V_m \times \sin wt}{V_{am}} = \sin wt \quad (1)$$

$$V_{b.pu} = \frac{V_m \times \sin (wt - 120^\circ)}{V_{bm}} = \sin (wt - 120^\circ) \quad (2)$$

$$V_{c.pu} = \frac{V_m \times \sin (wt + 120^\circ)}{V_{cm}} = \sin (wt + 120^\circ). \quad (3)$$

Table 1 The DSTATCOM device characters

DSTATCOM characters	Controlled rectified loads		
	R16L16	R20L20	R24L24
Capacitor V_{dc}	700 V	700 V	700 V
Capacitor C_{dc}	3000 uF	3000 uF	3000 uF
Interface inductor L_f	5 mH	5 mH	5 mH

The amplitude of the reference source current should cover the active power needed by the load and the losses of the power due to the switching process of the DSTATCOM thyristors. PI controller can be utilized to keep the DSTATCOM DC capacitor voltage at the reference value of 700 V by extracting the desired reference source current waves' amplitude by using Eqs. (4), (5):

$$V_{dcE(n)} = V_{dc}^* - V_{dcm(n)} \quad (4)$$

$$I_{Sp(n)}^* = I_{Sp(n-1)}^* + K_p (V_{dcE(n)} - V_{dcE(n-1)}) + K_i V_{dcE(n)}. \quad (5)$$

The proportional and integral constants utilized in this paper are $K_p = 0.65$ and $K_i = 10$.

The desired reference source current waves are the multiplying of the desired reference source amplitude into the desired reference source current phases as showing in Eqs. (6)–(8):

$$I_{Sa}^* = I_{Sp}^* \times V_{a.pu} = I_{Sp}^* \times \sin \omega t \quad (6)$$

$$I_{Sb}^* = I_{Sp}^* \times V_{b.pu} = I_{Sp}^* \times \sin(\omega t - 120^\circ) \quad (7)$$

$$I_{Sc}^* = I_{Sp}^* \times V_{c.pu} = I_{Sp}^* \times \sin(\omega t + 120^\circ). \quad (8)$$

Finally, the desired error signals to feed the hysteresis controller are extracted by comparing the desired reference source current waves with the sensed source current waves as Eqs. (9)–(11):

$$err_a = I_{Sa}^* - I_{Sam} \quad (9)$$

$$err_b = I_{Sb}^* - I_{Sbm} \quad (10)$$

$$err_c = I_{Sc}^* - I_{Scm}. \quad (11)$$

4.2 Type I fuzzy logic-based unit voltage template theory control algorithm

As Fig. 1 shows, the unit template strategy for controlling DSTATCOM device is wide explained with the detailed equations in [26]. The reference source current waves are generated to have the same phase as the source voltage waves by absorbing or injecting the reactive power to the controlled rectified load. Furthermore, the amplitude is extracted by the artificial controller to support the load with the necessary active power, and to supply the DSTATCOM device with active power needed to cover the losses in the IGBT switches and to charge the DC capacitor [26, 43].

In this paper, as Fig. 2 and Table 2, the Fuzzy Inference System (FIS) type utilized for T1FL controller is "Sugeno" with defuzzification method "wtaver". The type I fuzzy logic is function is to maintain the DC capacitor voltage at the reference-desired value of 700 V which stand for the "controlled" signal, which means that the two inputs should derived from controlled signal. For achieving this purpose, it has two input signals and one output signal. The first input is the difference between the DC capacitor reference value and the sensed value, which stands for the "error" signal, while the second input is the difference between the real value and the past value of first input, which stands for "change of error". The benefits of these two inputs to give information to the fuzzy logic controller if the controlled signal near to the reference value and if it is increasing or decreasing. Furthermore, while the unit voltage template strategy is used in this paper, so the output signal is the reference source current peak I_{Sp}^* . The benefit of the output signal is to change the value of the source current peak to keep the controlled signal at the desired value. The characteristics of the type I fuzzy logic

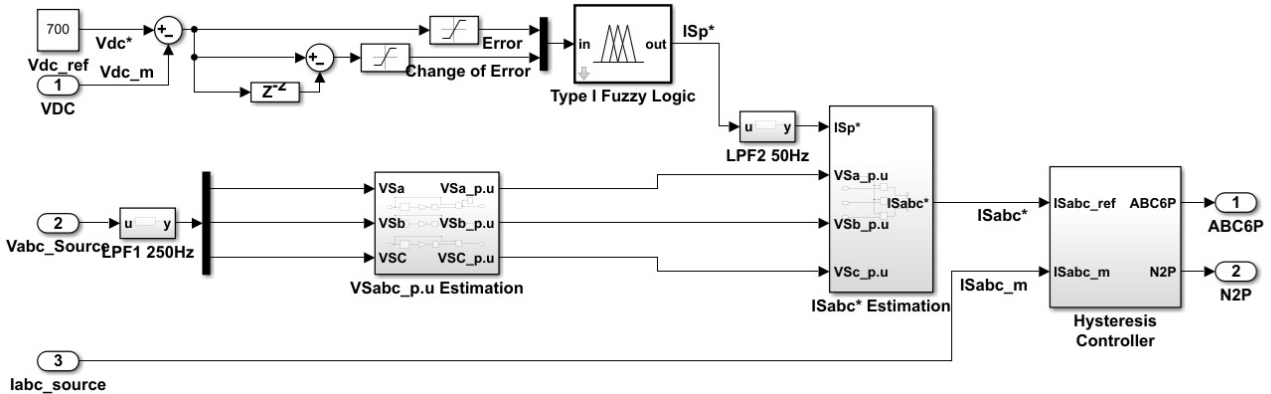


Fig. 1 T1FL-based UVT control strategy

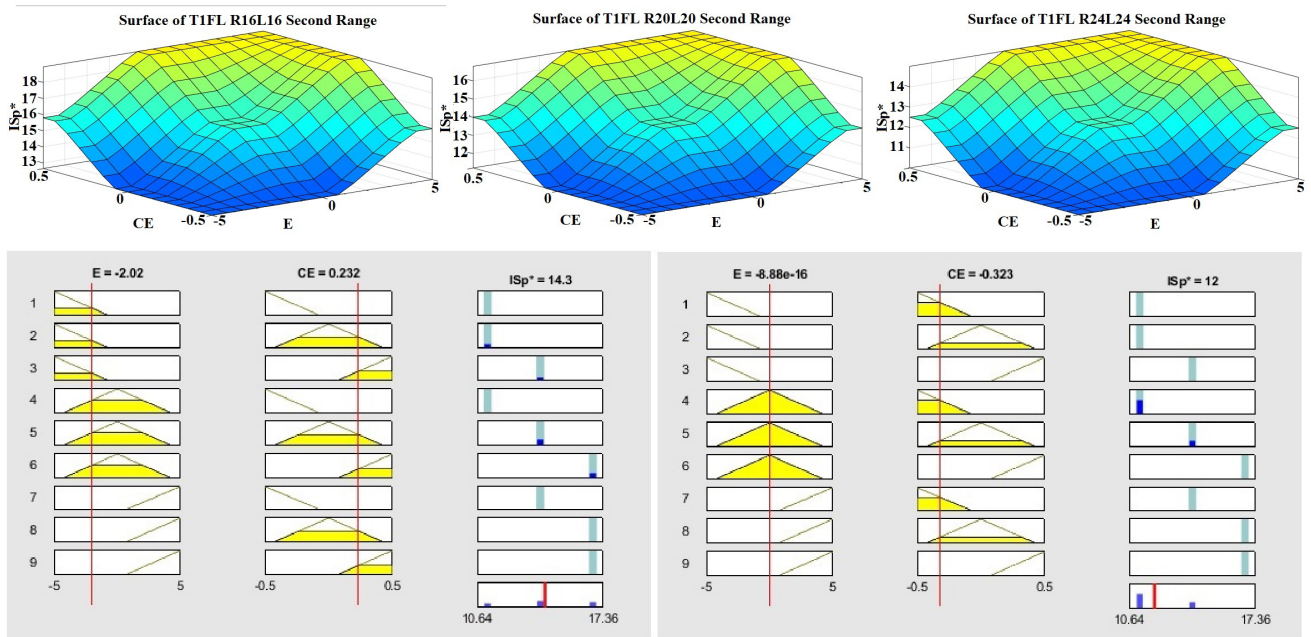


Fig. 2 Surface of type I fuzzy logic-based UVT tuned for controlled rectified loads $0.8 \text{ PF } R = 16 \Omega, L = 16 \text{ mH}, R = 20 \Omega, L = 20 \text{ mH}, R = 24 \Omega, L = 24 \text{ mH}$ with three membership functions second range of the two inputs. The Rule viewer of two examples shows the application of the nine rules on different values of inputs and the extracting the respect output values.

Table 2 Type I fuzzy logic controller-based unit voltage template strategy parameters

Controlled rectified load	T1FL controller based UVT strategy parameters		
	Error	Change of error	I_{sp}^* A
$R = 16 \Omega,$ $L = 16 \text{ mH}$	$[-2,2]$	$[-0.2,0.2]$	$[13,19]$
$R = 20 \Omega,$ $L = 20 \text{ mH}$	$[-2,2]$	$[-0.2,0.2]$	$[11,17]$
$R = 24 \Omega,$ $L = 24 \text{ mH}$	$[-2,2]$	$[-0.2,0.2]$	$[10,15]$

is as follows; the inputs use three membership functions with two different ranges, the output use three membership functions with one range, and the rule bases contain of nine rules. For the better results, the output range tuned to suit the three controlled rectified loads.

The nine rules utilized by the T1FL-based UVT (Table 3) consists of the logical statements in Algorithm 1 [25].

The Fig. 2 shows the surface of the T1FL based UVT with second range of input signals, tuned to suit the rectified load connected to the terminals of different situations of resistance in series with inductance. The surface is simply identified as three-dimensional mapping of the two inputs' values and the output's values. In the mentioned case above, the MATLAB program applies the inputs' values from the specific range $E [-5,5]$ $CE [-0.5,0.5]$ in the nine rules mentioned above, and then extract the output values from its specific range [11–17]. Then, the MATLAB

Table 3 Nine rules utilized by the T1FL-based UVT

CE/E	Low	Normal	High
Low	Low	Low	Normal
Normal	Low	Normal	High
High	Normal	High	High

Algorithm 1 Nine logical statements

1. If (E is Low) and (CE is Low) then (I_{sp}^* is Low)
2. If (E is Low) and (CE is Normal) then (I_{sp}^* is Low)
3. If (E is Low) and (CE is High) then (I_{sp}^* is Normal)
4. If (E is Normal) and (CE is Low) then (I_{sp}^* is Low)
5. If (E is Normal) and (CE is Normal) then (I_{sp}^* is Normal)
6. If (E is Normal) and (CE is High) then (I_{sp}^* is High)
7. If (E is High) and (CE is Low) then (I_{sp}^* is Normal)
8. If (E is High) and (CE is Normal) then (I_{sp}^* is High)
9. If (E is High) and (CE is High) then (I_{sp}^* is High)

program plot the extracted output values as a surface of three-dimensional mapping in the respect of the inputs' values. For example, if E is -2.02 and CE is 0.232 and after applying the nine rules then I_{sp}^* is 14.3 , another example, if E is -8.88×10^{-16} and CE is -0.323 and after applying the nine rules then I_{sp}^* is 12 .

As a results, in the surface view of T1FL R20L20, the respect output for the inputs $E -2.02$ and $CE 0.232$ is 14.3 , and the respect output for the inputs $E -8.88 \times 10^{-16}$ and $CE 0.323$ is 12 .

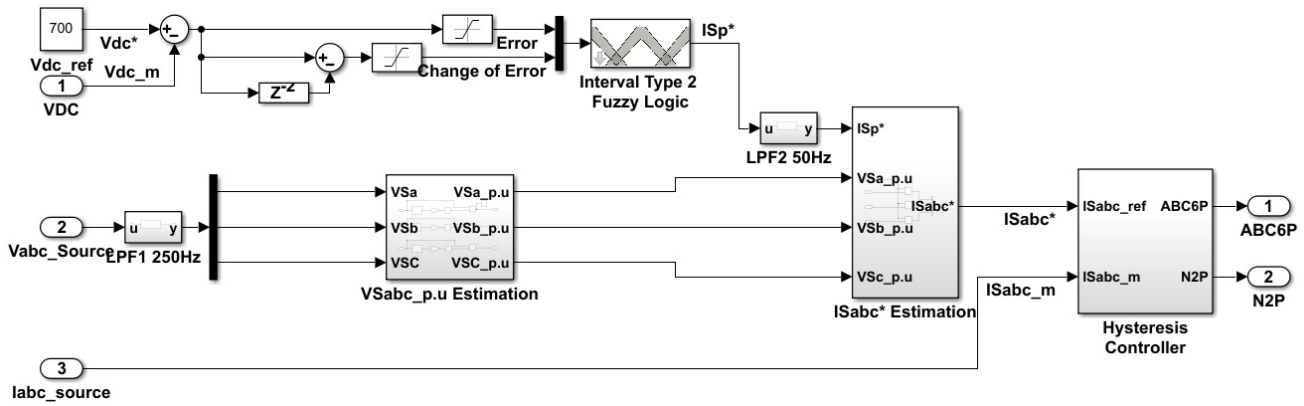


Fig. 3 IT2FL-based UVT control strategy

4.3 Interval type II fuzzy logic-based unit voltage template theory control algorithm

As Fig. 3 shows, the same unit voltage template strategy which utilized with type I fuzzy logic. It generates the reference source current signals and extracting the eight pulses needed to control the three-phase four-wire DSTATCOM device.

IT2FL considers as an artificial intelligence controller because it is utilizing the logic statements, as illustrated in the Table 4, to extract the output from the inputs not by applying mathematical equations. As Fig. 4 illustrated, the crisp values of the inputs are applied into the lower and upper input membership functions, and then transfer the crisp values into two fuzzy sets, because of using lower and upper input membership functions. Then after applying the rules on the IT2FSs inputs, the output will be extracted in IT2FSs. The type reduction utilized here to reduce the IT2FSs output into T1FSs, and this is the main deference between IT2FL and T1FL. Finally, the DE fuzzifier is used to transfer the output into the crisp value which be used by the controller.

As the Fig. 5 and Table 5 show, the main difference is the utilizing of IT2FL instead of the T1FL, to obtain the reference source current peak I_{sp}^* . The input signals have

Table 4 Nine rules utilized by the IT2FL-based UVT

CE/E	Low	Normal	High
Low	Low	Low	Normal
Normal	Low	Normal	High
High	Normal	High	High

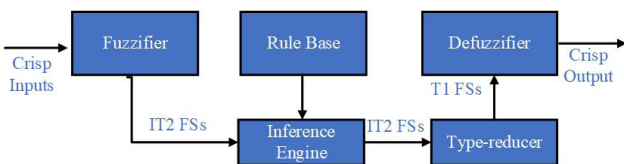


Fig. 4 Schematic diagram of IT2FL

three upper and lower membership functions with two different ranges. The output signal has three upper and lower membership functions with one range. The reason for the application of two input signals with different ranges to examine which range will give the better results. For the better results the output range is tuned to suit the three different controlled rectified loads.

5 Simulation and results

Fig. 6 is illustrated the examined low voltage grid with electrical source 415 V phase to phase, which supplying the controlled rectified load with three different situations of resistance and inductance connected to the terminal of the rectifier; 0.8 PF, $R = 16 \Omega$, $L = 16 \text{ mH}$, $R = 20 \Omega$, $L = 20 \text{ mH}$, $R = 24 \Omega$, $L = 24 \text{ mH}$. DSTATCOM device is used to enhance the PQ of the loads with two examined control algorithms; T1FL based UVT and IT2FL based UVT with two different ranges for the two inputs three membership functions. The examination of control strategies took place in MATLAB environment R2021a by using Fuzzy toolbox in the Simulink library, and the added Fuzzyt2 toolbox from official MATLAB website. The instruction how to add and to deal with Fuzzyt2 toolbox is explained in details in [51].

5.1 Controlled rectified loads

5.1.1 T1FL and IT2FL controllers with input signals of three MFs first range

In this situation, as Table 2 and Table 5 show, the application of three controllers PI, T1FL and IT2FL with the UVT control strategy to control DSTATCOM device. The examined controlled rectified load has three values of resistance and inductance connected in series between its terminals; $R = 16 \Omega$, $L = 16 \text{ mH}$, $R = 20 \Omega$, $L = 20 \text{ mH}$, $R = 24 \Omega$, $L = 24 \text{ mH}$ with the same firing angel $\alpha = 30^\circ$ and 0.8 PF. The applied T1FL and IT2FL have two inputs with three

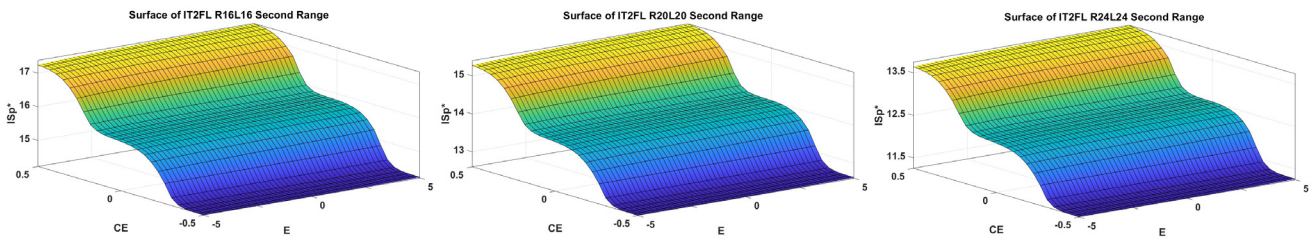


Fig. 5 Surface of interval IT2FL-based UVT tuned for controlled rectified loads $0.8 \text{ PF } R = 16 \Omega, L = 16 \text{ mH}, R = 20 \Omega, L = 20 \text{ mH}, R = 24 \Omega, L = 24 \text{ mH}$ with three membership functions second range of the two inputs.

Table 5 IT2FL-based UVT strategy parameters

Controlled rectified load	IT2FL based UVT parameters			
	Upper/Lower MF	Error	Change of error	$I_{sp}^* \text{ A}$
$R = 16 \Omega$ $L = 16 \text{ mH}$	U MF	$[-2,2,1]$	$[-0.2,0.2,1]$	$[13,19,1]$
	L MF	$[-2,2,0.5]$	$[-0.2,0.2,0.5]$	$[13,19,0.5]$
	U MF	$[-5,5,1]$	$[-0.5,0.5,1]$	$[13,19,1]$
	L MF	$[-5,5,0.5]$	$[-0.5,0.5,0.5]$	$[13,19,0.5]$
$R = 20 \Omega$ $L = 20 \text{ mH}$	U MF	$[-2,2,1]$	$[-0.2,0.2,1]$	$[11,17,1]$
	L MF	$[-2,2,0.5]$	$[-0.2,0.2,0.5]$	$[11,17,0.5]$
	U MF	$[-5,5,1]$	$[-0.5,0.5,1]$	$[11,17,1]$
	L MF	$[-5,5,0.5]$	$[-0.5,0.5,0.5]$	$[11,17,0.5]$
$R = 24 \Omega$ $L = 24 \text{ mH}$	U MF	$[-2,2,1]$	$[-0.2,0.2,1]$	$[10,15,1]$
	L MF	$[-2,2,0.5]$	$[-0.2,0.2,0.5]$	$[10,15,0.5]$
	U MF	$[-5,5,1]$	$[-0.5,0.5,1]$	$[10,15,1]$
	L MF	$[-5,5,0.5]$	$[-0.5,0.5,0.5]$	$[10,15,0.5]$

MFs first range of $[-2,2]$ for the first input signal E and $[-0.2,0.2]$ of the second input signal CE ; while the output signal has three different ranges for each load situations.

As Table 6 and Table 7 show, the results cover the controlled signal response characteristics of RT, PT, ST and OS; the electrical source parameter I_s -THD (electrical source current total harmonic distortion), P_s , Q_s and S -PF (source power factor); for the three controlled rectified load situations with the mentioned controllers to conclude which the best controllers between them.

First, as Fig. 7 shows, at the controlled rectified load with resistance and inductor connected in series between its terminals $R = 16 \Omega, L = 16 \text{ mH}, \alpha = 30^\circ, 0.8 \text{ PF}$; the IT2FL controller based UVT Strategy with inputs first range has; the DC capacitor voltage wave response as $RT = 7.8 \text{ s}, PT = 14.9 \text{ s}, ST = 50 \text{ s}$ which is as same as the T1FL with UVT strategy and better than PI controller with UVT Strategy, see Table 6; the electrical source current with total harmonic distortion of 3.04% which is better than both T1FL controller and PI controller respectively 3.21% 3.35%, see Table 7; the electrical source power factor of 0.98 which is as same as the T1FL and PI controller.

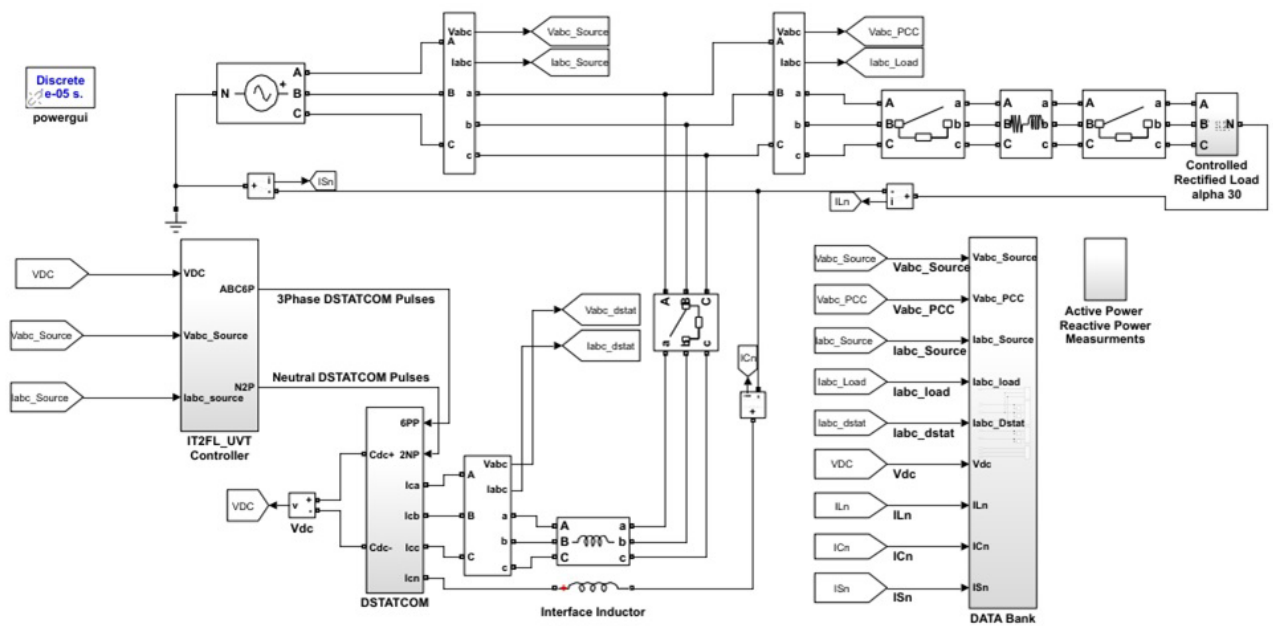


Fig. 6 The examined electrical grid which is supplying the controlled rectified load, DSTATCOM device is connected in shunt with load and controlled by UVT-T2FL control strategy.

Table 6 The comparison of response parameters of controlled capacitor DC voltage signal at different controlled rectified load scenarios with input signals of three MFs first range

Controller	Controlled rectified load 0.8 PF	Capacitor DC voltage parameter				
		RT mS	PT mS	ST mS	OS %	Peak V
UVT_PI	$R = 16 \Omega$	6.4	31.5	200	12.5%	787
UVT_T1FL	$L = 16 \text{ mH}$	7.8	14.9	50	0.28%	702
UVT_T2FL	$\alpha = 30^\circ$	7.8	14.9	50	0.28%	702
UVT_PI	$R = 20 \Omega$	6.4	31.5	200	13%	791
UVT_T1FL	$L = 20 \text{ mH}$	7.8	14.8	50	0%	700
UVT_T2FL	$\alpha = 30^\circ$	7.8	14.8	50	0%	700
UVT_PI	$R = 24 \Omega$	6.4	31.5	200	13.2%	793
UVT_T1FL	$L = 24 \text{ mH}$	7.8	14.7	50	0%	700
UVT_T2FL	$\alpha = 30^\circ$	7.8	14.7	50	0%	700

Table 7 The comparison of electrical source parameters THD and Source PF at different controlled rectified loads with input signals of three MFs first range

Controller	Controlled rectified load 0.8 PF	Electrical source parameter			
		Is-THD	Ps W	Qs Var	S-PF
UVT_PI	$R = 16 \Omega$	3.35%	8250	1600	0.98
UVT_T1FL	$L = 16 \text{ mH}$	3.21%	8250	1600	0.98
UVT_T2FL	$\alpha = 30^\circ$	3.04%	8250	1600	0.98
UVT_PI	$R = 20 \Omega$	3.47%	7350	1400	0.98
UVT_T1FL	$L = 20 \text{ mH}$	3.38%	7350	1400	0.98
UVT_T2FL	$\alpha = 30^\circ$	3.35%	7350	1400	0.98
UVT_PI	$R = 24 \Omega$	3.81%	6580	1250	0.98
UVT_T1FL	$L = 24 \text{ mH}$	3.69%	6580	1250	0.98
UVT_T2FL	$\alpha = 30^\circ$	3.64%	6580	1250	0.98

Second, as Fig. 8 shows, at the controlled rectified load with resistance and inductor connected in series between its terminals $R = 20 \Omega$, $L = 20 \text{ mH}$, $\alpha = 30^\circ$ 0.8 PF; the IT2FL controller based UVT Strategy with inputs first range has; the DC capacitor voltage wave response as $RT = 7.8 \text{ s}$, $PT = 14.8 \text{ s}$, $ST = 50 \text{ s}$ which is as same as the T1FL with UVT strategy and better than PI controller with UVT Strategy, see Table 6; the electrical source current with total harmonic distortion of 3.35% which is better than both T1FL controller and PI controller respectively 3.38% 3.47%, see Table 7; the electrical source power factor of 0.98 which is as same as the T1FL and PI controller.

Third, as Fig. 9 shows, at the controlled rectified load with resistance and inductor connected in series between its terminals $R = 24 \Omega$, $L = 24 \text{ mH}$, $\alpha = 30^\circ$, 0.8 PF; the IT2FL controller based UVT Strategy with inputs first range has; the DC capacitor voltage wave response as $RT = 7.8 \text{ s}$, $PT = 14.9 \text{ s}$, $ST = 50 \text{ s}$ which is as same as the T1FL with UVT strategy and better than PI controller with UVT Strategy, see Table 6; the electrical source current with total harmonic distortion of 3.64% which is better than both T1FL controller and PI controller respectively 3.69% 3.81%, see Table 7; the electrical source power factor of 0.98 which is as same as the T1FL and PI controller.

The utilization of the new intelligence IT2FL controller based UVT control strategy with the first input signals range and specified output signal range for each load situations improve the DC capacitor voltage response in the same way of the old intelligence T1FL, and improve the source current wave total harmonic distortion in better way of the old intelligence T1FL with all different controller rectified loads.

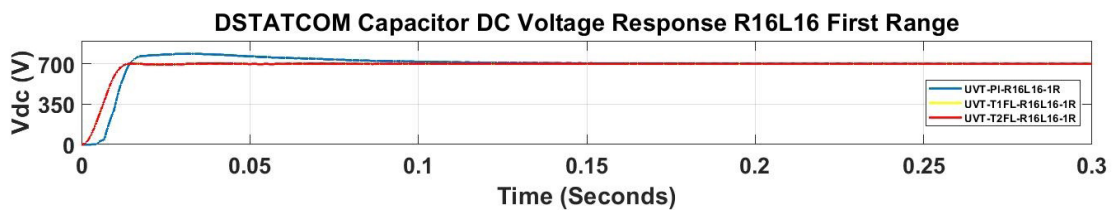


Fig. 7 DSTATCOM capacitor DC voltage response is shown at controlled rectified load 0.8 PF $R = 16 \Omega$, $L = 16 \text{ mH}$ with input signals of three MFs first range.

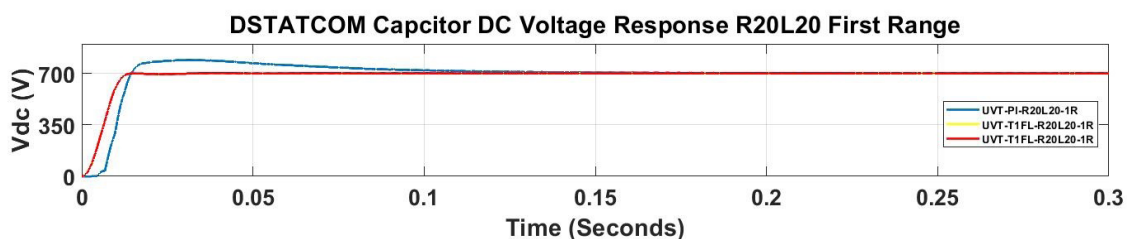


Fig. 8 DSTATCOM capacitor DC voltage response is shown at controlled rectified load 0.8 PF $R = 20 \Omega$, $L = 20 \text{ mH}$ with input signals of three MFs first range.

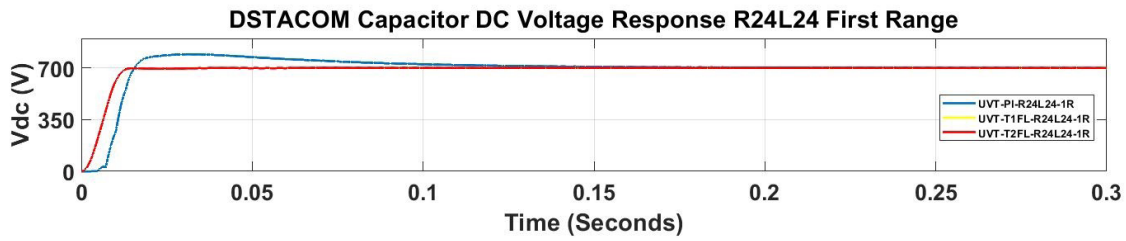


Fig. 9 DSTACOM capacitor DC voltage response is shown at controlled rectified load 0.8 PF , $R = 24 \Omega$, $L = 24 \text{ mH}$ with input signals of three MFs first range.

5.1.2 T1FL and IT2FL controllers with input signals of three MFs second range

In this situation, as Table 2 and Table 5 show, the application of three controllers PI, T1FL and IT2FL with the UVT control strategy to control DSTACOM device. The examined controlled rectified load has three values of resistance and inductance connected in series between its terminals; $R = 16 \Omega$, $L = 16 \text{ mH}$, $R = 20 \Omega$, $L = 20 \text{ mH}$, $R = 24 \Omega$, $L = 24 \text{ mH}$ with the same firing angle $\alpha = 30^\circ$ and 0.8 PF . The applied T1FL and IT2FL have two inputs with three MFs second range of $[-5,5]$ for the first input signal E and $[-0.5,0.5]$ of the second input signal CE ; while the output signal has three different ranges for each load situations.

As Table 8 and Table 9 show, the results cover the controlled signal response characteristics of RT, PT, ST and OS; the electrical source parameter $I_s\text{-THD}$, P_s , Q_s and $S\text{-PF}$; for the three controlled rectified load situations with the mentioned controllers to conclude which the best controllers between them.

First, as Fig. 10 shows, at the controlled rectified load with resistance and inductor connected in series between its terminals $R = 16 \Omega$, $L = 16 \text{ mH}$, $\alpha = 30^\circ$, 0.8 PF ; the IT2FL controller based UVT Strategy with inputs second

Table 8 The comparison of response parameters of controlled capacitor DC voltage signal at different controlled rectified load scenarios with input signals of three MFs second range

Controller	Controlled rectified load 0.8 PF	Capacitor DC voltage parameter				
		RT mS	PT mS	ST mS	OS %	Peak V
UVT_PI	$R = 16 \Omega$	6.4	31.5	200	12.5%	787
UVT_T1FL	$L = 16 \text{ mH}$	7.8	14.9	50	0.28%	702
UVT_T2FL	$\alpha = 30^\circ$	7.8	14.9	50	0.28%	702
UVT_PI	$R = 20 \Omega$	6.4	31.5	200	13%	791
UVT_T1FL	$L = 20 \text{ mH}$	7.9	14.8	50	0%	700
UVT_T2FL	$\alpha = 30^\circ$	7.9	14.8	50	0%	700
UVT_PI	$R = 24 \Omega$	6.4	31.5	200	13.2%	793
UVT_T1FL	$L = 24 \text{ mH}$	7.9	14.7	50	0%	700
UVT_T2FL	$\alpha = 30^\circ$	7.9	14.7	50	0%	700

Table 9 The comparison of electrical source parameters THD and Source PF at different controlled rectified loads with input signals of three MFs second range

Controller	Controlled rectified load 0.8 PF	Electrical source parameter			
		$I_s\text{-THD}$	P_s W	Q_s Var	$S\text{-PF}$
UVT_PI	$R = 16 \Omega$	3.35%	8250	1600	0.98
UVT_T1FL	$L = 16 \text{ mH}$	2.99%	8250	1600	0.98
UVT_T2FL	$\alpha = 30^\circ$	2.98%	8250	1600	0.98
UVT_PI	$R = 20 \Omega$	3.47%	7350	1400	0.98
UVT_T1FL	$L = 20 \text{ mH}$	3.34%	7350	1400	0.98
UVT_T2FL	$\alpha = 30^\circ$	3.30%	7350	1400	0.98
UVT_PI	$R = 24 \Omega$	3.81%	6580	1250	0.98
UVT_T1FL	$L = 24 \text{ mH}$	3.64%	6580	1250	0.98
UVT_T2FL	$\alpha = 30^\circ$	3.63%	6580	1250	0.98

range has; the DC capacitor voltage wave response as $RT = 7.8 \text{ s}$, $PT = 14.9 \text{ s}$, $ST = 50 \text{ s}$ which is as same as the IT2FL controller based UVT Strategy with inputs first range, see Table 8; the electrical source current with total harmonic distortion of 2.98% which is better than IT2FL controller based UVT Strategy with inputs first range 3.04%, see Table 9; the electrical source power factor of 0.98 which is as same as IT2FL controller based UVT Strategy with inputs first range.

Second, as Fig. 11 shows, at the controlled rectified load with resistance and inductor connected in series between its terminals $R = 20 \Omega$, $L = 20 \text{ mH}$, $\alpha = 30^\circ$, 0.8 PF ; the IT2FL controller based UVT Strategy with inputs second range has; the DC capacitor voltage wave response as $RT = 7.8 \text{ s}$, $PT = 14.8 \text{ s}$, $ST = 50 \text{ s}$ which is as same as the IT2FL controller based UVT Strategy with inputs first range, see Table 8; the electrical source current with total harmonic distortion of 3.30% which is better than IT2FL controller based UVT Strategy with inputs first range 3.35%, see Table 9; the electrical source power factor of 0.98 which is as same as IT2FL controller based UVT Strategy with inputs first range. The Fast Fourier transfer of the load current and source current with three different controllers are illustrated in Fig. 12.

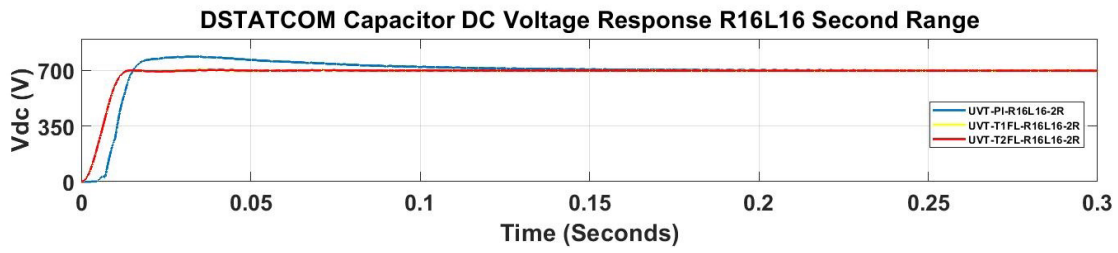


Fig. 10 DSTATCOM capacitor DC voltage response is shown at controlled rectified load 0.8 PF $R = 16 \Omega$, $L = 16$ mH with input signals of three MFs second range.

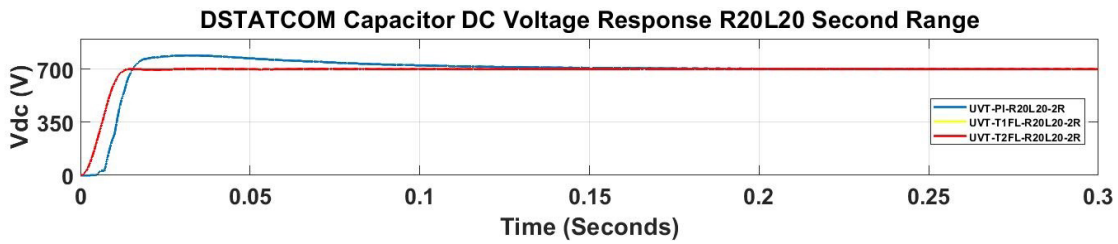


Fig. 11 DSTATCOM capacitor DC voltage response is shown at controlled rectified load 0.8 PF $R = 20 \Omega$, $L = 20$ mH with input signals of three MFs second range.

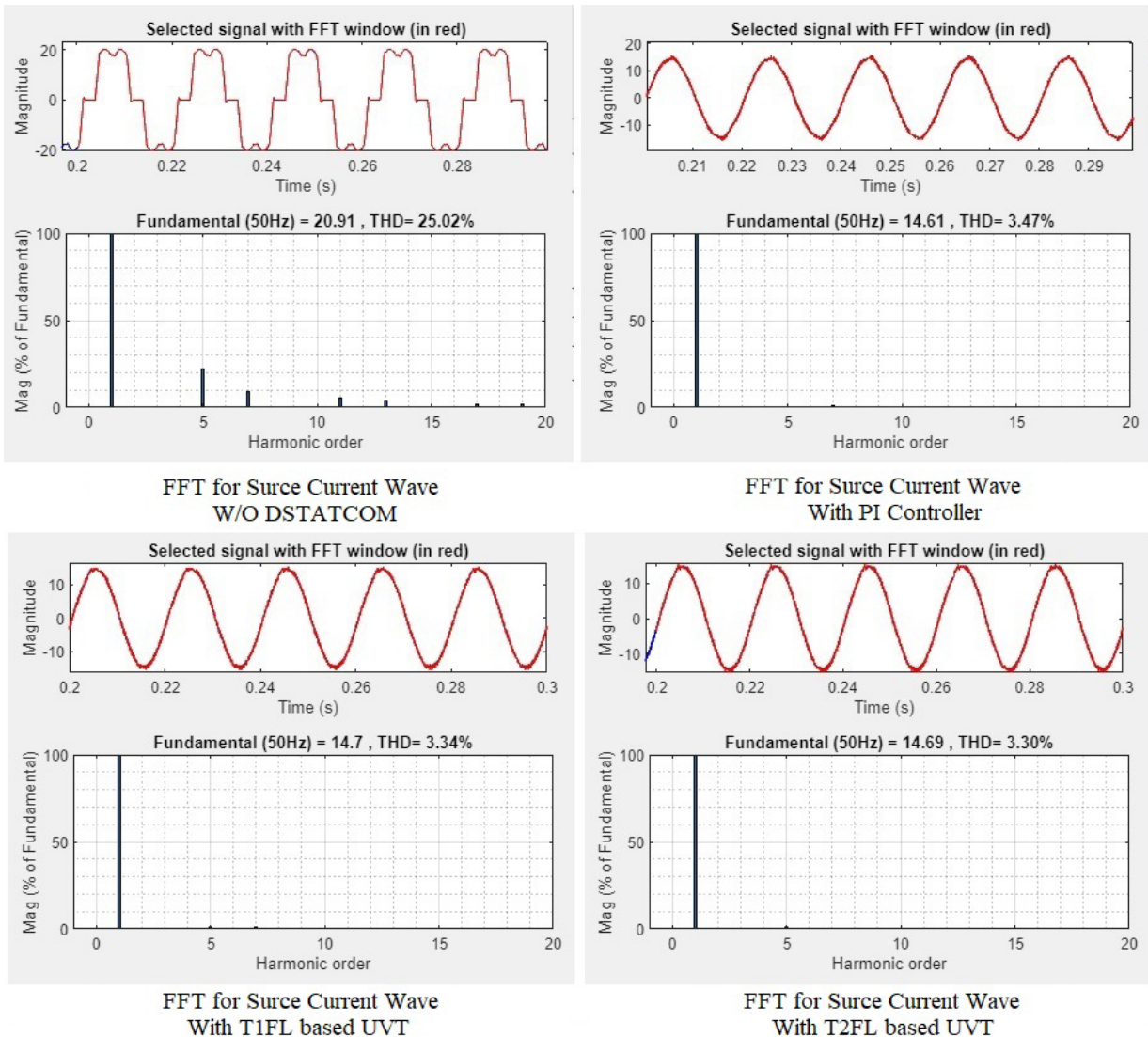


Fig. 12 FFT for source current with different controller with second range at controlled rectified load with $R = 20$, $L = 20$ mH

Third, as Fig. 13 shows, at the controlled rectified load with resistance and inductor connected in series between its terminals $R = 24 \Omega$, $L = 24 \text{ mH}$, $\alpha = 30^\circ$ 0.8 PF; the IT2FL controller based UVT Strategy with inputs second range has; the DC capacitor voltage wave response as $RT = 7.8 \text{ s}$, $PT = 14.7 \text{ s}$, $ST = 50 \text{ s}$ which is as same as the IT2FL controller based UVT Strategy with inputs first range, see Table 8; the electrical source current with total harmonic distortion of 3.63% which is better than IT2FL controller based UVT Strategy with inputs first range 3.64%, see Table 9; the electrical source power factor of 0.98 which is as same as IT2FL controller based UVT Strategy with inputs first range.

The utilization of the IT2FL controller based UVT control strategy with the input signals second range and specified output signal range for each load situations improve the DC capacitor voltage response in the same way of the IT2FL controller based UVT control strategy with the input signals first range, and improve the source current wave total harmonic distortion in better way of the IT2FL controller based UVT control strategy with the input signals first range with all different controller rectified loads.

In Fig. 14, the DSTATCOM device with the new intelligence IT2FL controller based UVT with input signals second range begin to compensate at the $t = 0.1 \text{ s}$ to improve the PQ of the source current waves of the controlled rectified load with resistance and inductor connected in series between its terminals. First, between the time $t = [0, 0.1] \text{ s}$, there is no compensating current, so the source current waves have the same shape of the deformed load current waves, and there is a phase between the voltage and source current waves. In the other hand, between the time $t = [0.1, 0.5] \text{ s}$, the compensating current eliminate the harmonics in the load current waves, so the source current waves have a pure sinusoidal shape, and there is no phase between the voltage and source current waves.

In Fig. 15, between the time $t = [0, 0.1] \text{ s}$, the source was providing the controlled rectified load with the reactive power which makes the source power factor at the value

of 0.8. Between the time $t = [0.1, 0.5] \text{ s}$, the DSTATCOM device starts to provide the controlled rectified load with the reactive power which improve the power factor of the source to the value of 0.98.

5.2 Different loads and disturbances with controlled rectified load

This situation examines the new intelligence IT2FL based UVT control strategy with input signals three MFs second range with different load situation and disturbances of the controlled rectified load. The different loads are normal load 20 A, decrement of load 17 A and increment of load 23 A. While the disturbances are unbalanced load in one phase A, unbalanced load in phase B and phase C and the voltage swell 0.8 p.u. As Fig. 16, Fig. 17 and Fig. 18 illustrate; between the time $t = [0-0.4] \text{ s}$, the normal controlled rectified load peak current value is almost 20 A; between the time $t = [0.4-0.6] \text{ s}$, there is an unbalanced load in the phase A; between the time $t = [0.6-0.8] \text{ s}$, there is decrement of the controlled rectified load peak current to the value 17 A; between the time $t = [0.8-1] \text{ s}$, there is an unbalanced load in the phase B and phase C; between the time $t = [1-1.2] \text{ s}$, there is an increment of the controlled rectified load peak current to the value 23 A; between the time $t = [1.2-1.4] \text{ s}$, there is voltage swell in the point of common coupling voltage by the value of 0.8 p.u.

As Table 10 and Table 11 show, the results cover the controlled signal response characteristics of RT, PT, ST and OS; The electrical source parameter S-THD, Ps, Qs and S-PF; for different loads and disturbances with the mentioned controllers to conclude which the best controllers between them.

As the Table 10 and Fig. 17 show, for the DSTATCOM DC capacitor voltage response, the IT2FL and TIFL have the same response as a rising time 7.9 ms, peak time of 14.8 ms and settling time 50 ms with no overshoot; in comparison with PI controller with the response as rising time 6.4 ms, peak time 31.5 ms and settling time 200 ms with 13% overshoot.

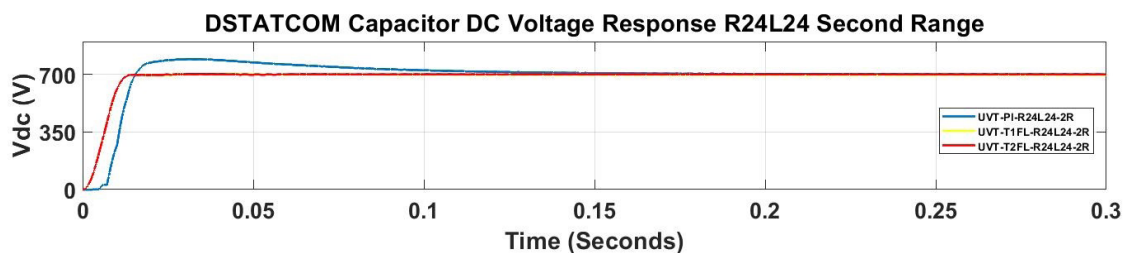


Fig. 13 DSTATCOM capacitor DC voltage response is shown at controlled rectified load 0.8 PF $R = 24 \Omega$, $L = 24 \text{ mH}$ with input signals of three MFs second range.

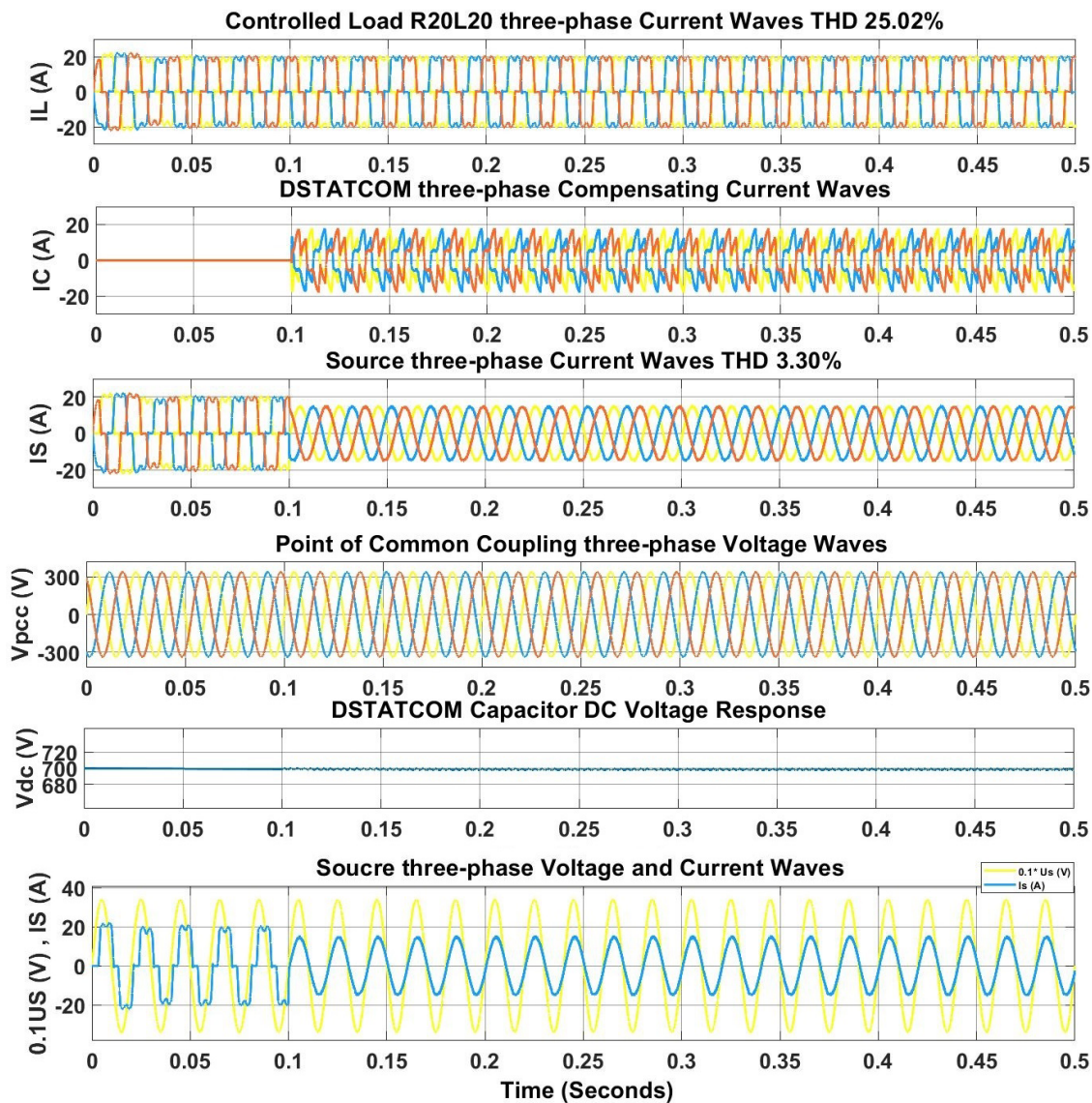


Fig. 14 Signals' waveforms of the examined electrical grid are shown at controlled rectified load 0.8 PF $R = 20 \Omega$, $L = 20 \text{ mH}$ while using UVT_T2FL with input signals of three MFs second range based on DSTATCOM device. At $t = 0.1 \text{ s}$, the compensation process starts.

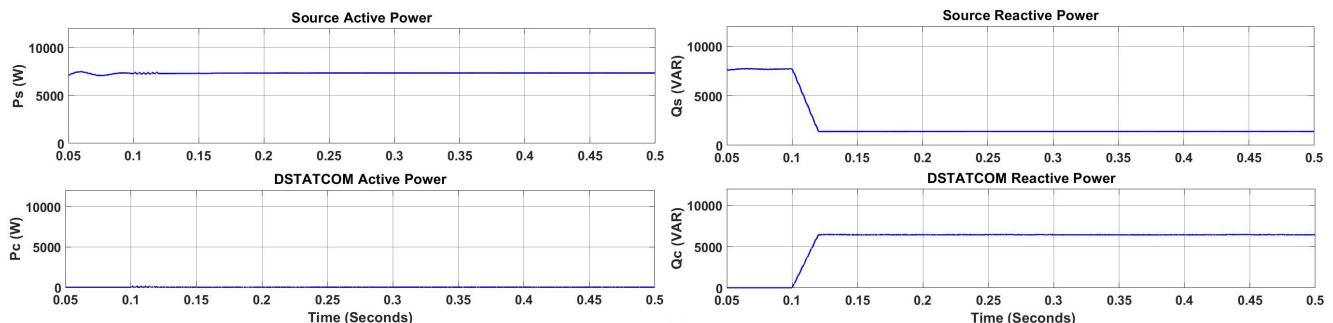


Fig. 15 The different power types of electrical source and DSTATCOM are shown at controlled rectified load 0.8 PF $R = 20 \Omega$, $L = 20 \text{ mH}$ while using UVT_T2FL with input signals of three MFs second range based on DSTATCOM.

On the other hand, as the Table 11, Fig. 16 and Fig. 18 show, for the electrical source parameters, the IT2FL based UVT gives the best THD mitigation in the different loads

and disturbances situation in comparison with PI and T1FL based UVT. First, the normal load of 20 A between time $0\text{--}0.4 \text{ s}$, the IT2FL improves the source current THD to the

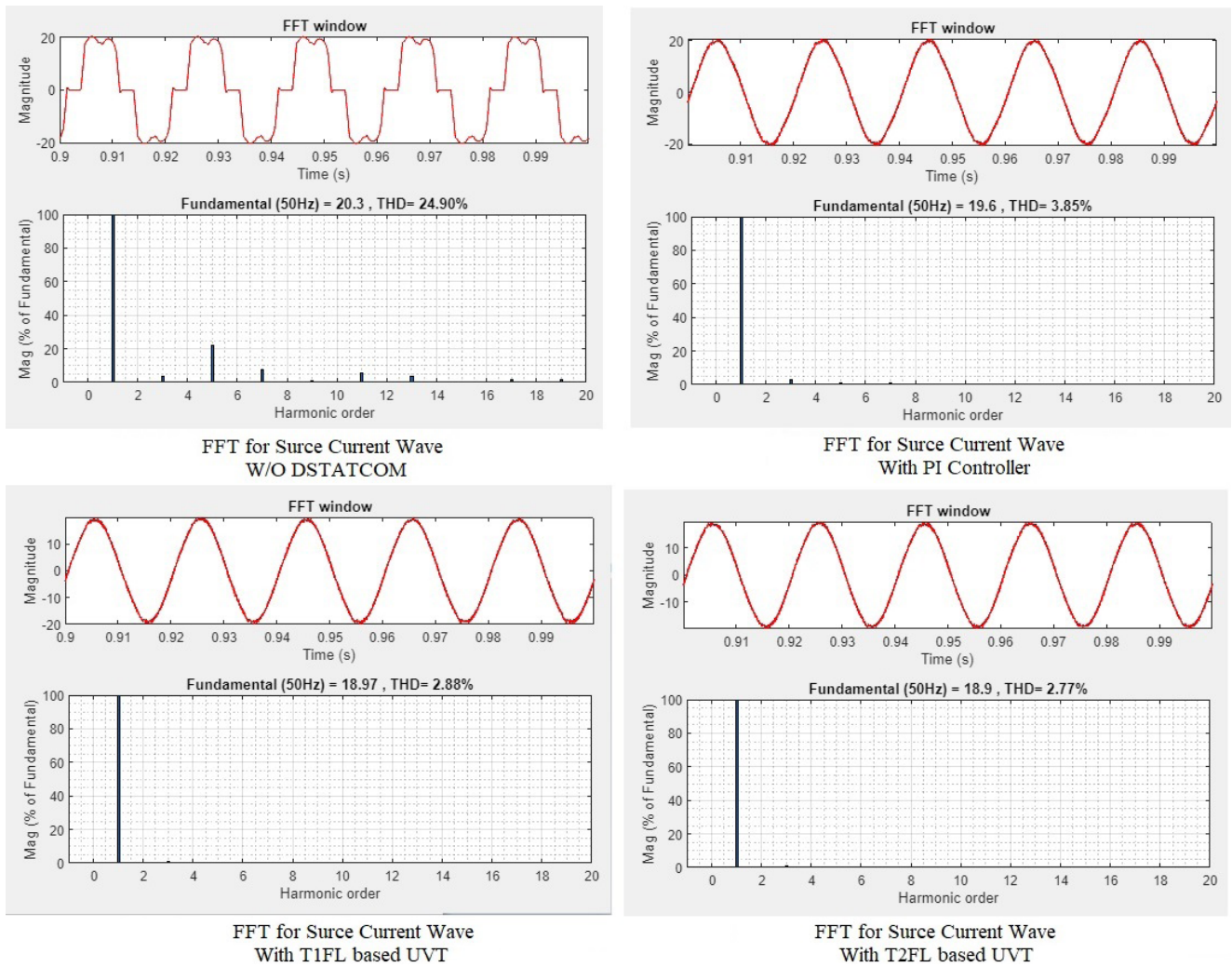


Fig. 16 FFT for source current with different controller with second range at controlled rectifier load with unbalanced load two phases between 0.8–1.00 s

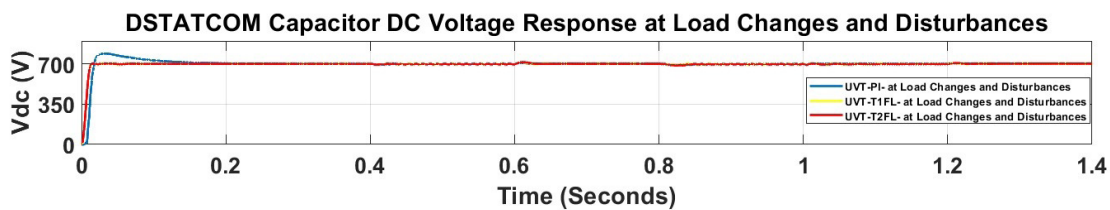


Fig. 17 DSTATCOM capacitor DC voltage response is shown at controlled rectified load with load changes and disturbances.

value of 3.30% in comparison with T1FL with 3.34% and PI with 3.47%. Second, the unbalanced load in phase A between time 0.4–0.6 s, the IT2FL improves the source current THD to the value of 2.96% in comparison with T1FL with 3.35% and PI with 4.52%. Third, the load decrement 17 A between 0.6–0.8 s, the IT2FL improves the source current THD to the value of 3.66% in comparison with T1FL with 3.70% and PI with 3.86%. Fourth, as Fig. 17 shows, the unbalanced load in phase B and phase C, the IT2FL improves the source current THD to the value of 2.77% in comparison with T1FL with 2.88% and PI with 3.85%. fifth, the load increment

23 A, the IT2FL improves the source current THD to the value of 3.12% in comparison with T1FL with 3.23% and PI with 3.31%. Sixth, the voltage swell, the IT2FL improves the source current THD to the value of 3.99% in comparison with T1FL with 4.01% and PI with 4.40%.

The new technique of IT2FL based UVT with the input signals three MFs second range keeps the source current waves at the sinusoidal shape and with the same phase with voltage current waves, it gives the best harmonics mitigation of the source current wave at different loads and disturbances situation in comparison with the other

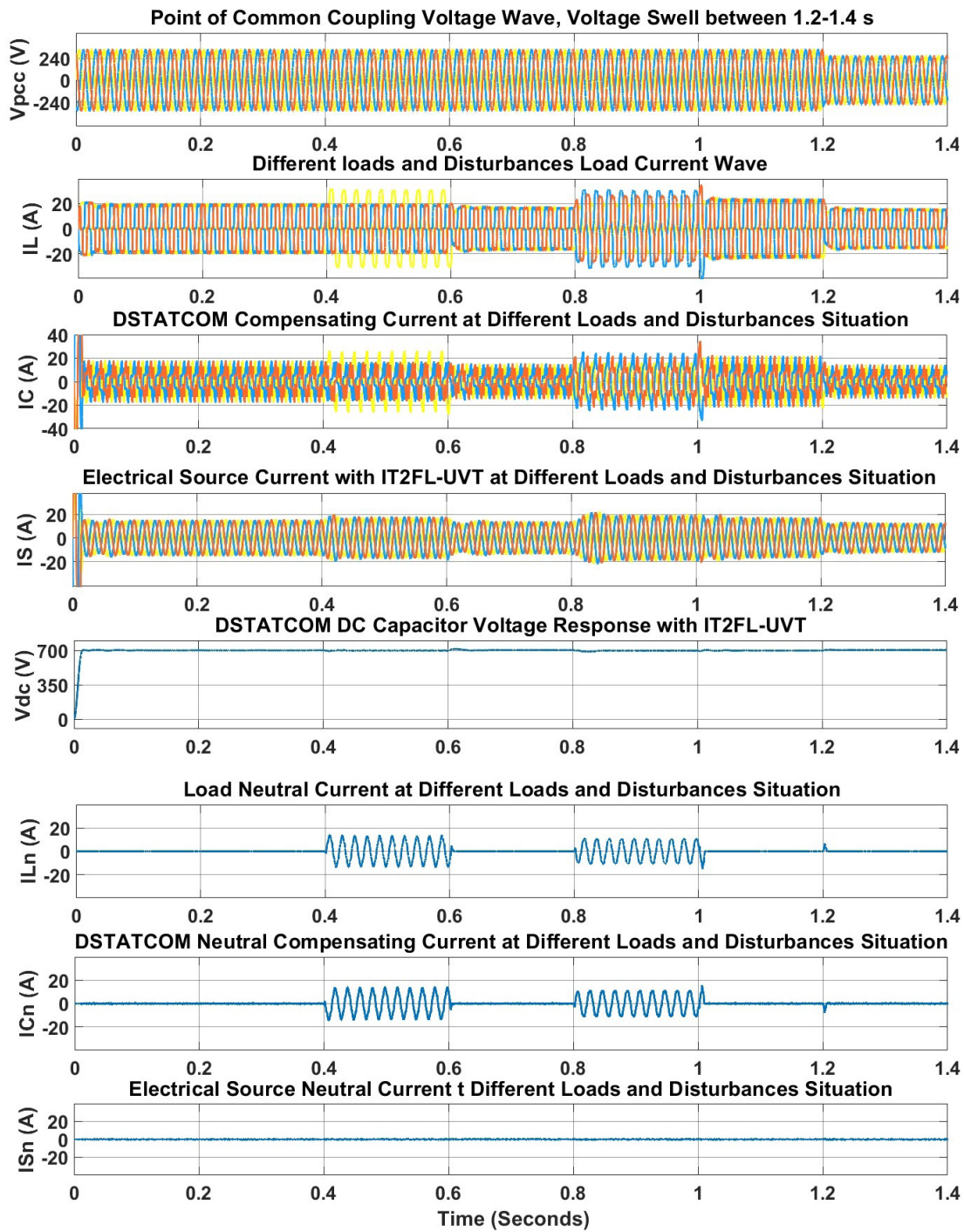


Fig. 18 Electrical grid parameters are shown with UVT-T2FL with input signals of three MFs second range based on DSTATCOM device at different loads and disturbances with controlled rectified. First normal load is between 0–0.4 s, unbalanced load one phase is between 0.4–0.6 s, load decrement is between 0.6–0.8 s, unbalanced load two phases is between 0.8–1.00 s, load increment is between 1.00–1.2 s and voltage swell is between 1.2–1.4 s.

Table 10 The capacitor DC voltage response at different loads and disturbances with controlled

Controller	Capacitor DC voltage parameter				
	RT mS	PT mS	ST mS	OS %	Peak V
UVT_PI	6.4	31.5	200	13%	791
UVT_T1FL	7.9	14.8	50	0%	700
UVT_T2FL	7.9	14.8	50	0%	700

controllers. It also keeps the DC capacitor voltage wave at the desired value for reference at 700 V in load changes and disturbances situation.

6 Conclusion

The recent intelligent interval type II fuzzy logic controller is utilized with the unit voltage template control

Table 11 The comparison of electrical source parameters THD and Source PF at different loads and disturbances

Controller	Different loads and disturbances with controlled rectified load											
	Normal load 20 A 0–0.4 s		Unbalanced load one phase 0.4–0.6 s		Load decrement 17 A 0.6–0.8 s		Unbalanced load two phases 0.8–1 s		Load increment 23 A 1–1.2 s		Voltage swell 0.8 p.u. 1.2–1.4 s	
	Is-THD	S-PF	Is-THD	S-PF	Is-THD	S-PF	Is-THD	S-PF	Is-THD	S-PF	Is-THD	S-PF
WO/DSTATCOM	25.08%	0.8	25.06%	0.8	25.89%	0.8	24.90%	0.8	23.80%	0.8	24.99%	0.8
UVT_PI	3.47%	0.98	4.52%	0.98	3.86%	0.98	3.85%	0.98	3.31%	0.98	4.40%	0.98
UVT_TIFL	3.34%	0.98	3.35%	0.98	3.70%	0.98	2.88%	0.98	3.23%	0.98	4.01%	0.98
UVT_T2FL	3.30%	0.98	2.96%	0.98	3.66%	0.98	2.77%	0.98	3.12%	0.98	3.99%	0.98

strategy to control DSTATCOM device in the electrical grid which supplying controlled rectified load. According to the results, the main contributions of this paper:

1. Tuning process of the IT2FL controller based UVT to suit the different values of controlled rectified loads.
2. Two ranges for the input signals with three MFs succeeds in improving the shape of deformed source current waves to the sinusoidal shape and keep them at the same phase of the source voltage waves.

3. The new intelligent IT2FL based UVT with the input signals three MFs second range succeeds in improving the deformed source current waves better than TIFL based UVT and better than IT2FL based UVT with the input signals three MFs first range.
4. The new intelligent IT2FL based UVT does the desired task in enhancing the shape of source current waves in the situation of different loads and disturbances.

References

- [1] Hossain, E., Tür, M. R., Padmanaban, S., Ay, S., Khan, I. "Analysis and Mitigation of Power Quality Issues in Distributed Generation Systems Using Custom Power Devices", *IEEE Access*, 6, pp. 16816–16833, 2018. <https://doi.org/10.1109/ACCESS.2018.2814981>
- [2] Zhao, Y. "Electrical Power Systems Quality", University of Buffalo, New York, NY, USA, 2016. [online] Available at: <https://www.scribd.com/document/357088104/Power-Quality-Intro> [Accessed: 04 March 2023]
- [3] Secui, D. C., Dziñac, S., BENDEA, G. V., Dziñac, I. "An ACO Algorithm for Optimal Capacitor Banks Placement in Power Distribution Networks", *Studies in Informatics and Control*, 18(4), pp. 305–314, 2009.
- [4] Finlay, G. S. "IEC 555 part 2-harmonics: background and implications", In: *IEE Colloquium on Single-Phase Supplies: Harmonic Regulations and Remedies*, London, UK, 1991, pp. 2/1–2/9.
- [5] IEEE "IEEE Std 519-1992 - IEEE Recommended Practice and Requirements for Harmonics Control in Electric Power Systems", IEEE, 1993. <https://doi.org/10.1109/IEEESTD.1993.114370>
- [6] IEC "IEC 61000-3-2:2014 Electromagnetic compatibility (EMC) – Part 3-2: Limits - Limits for harmonic current emissions (equipment input current ≤16 A per phase)", International Electrotechnical Commission, Geneva, Switzerland, 2014.
- [7] Lee, W.-J., Son, Y., Ha, J.-I. "Single-phase active power filtering method using diode-rectifier-fed motor drive", *IEEE Transactions on Industry Applications*, 51(3), pp. 2227–2236, 2015. <https://doi.org/10.1109/TIA.2014.2365629>
- [8] Rönnerberg, S. "Power line communication and customer equipment", Licentiate Thesis, Luleå University of Technology, 2011.
- [9] Amaripadath, D., Roche, R., Joseph-Auguste, L., Istrate, D., Fortune, D., Braun, J. P., Gao, F. "Power quality disturbances on smart grids: Overview and grid measurement configurations", In: *2017 52nd International Universities Power Engineering Conference (UPEC)*, Heraklion, Greece, 2017, pp. 1–6. ISBN 978-1-5386-2345-9 <https://doi.org/10.1109/UPEC.2017.8231975>
- [10] Kaddah, S. S., Abo-Al-Ez, K. M., Megahed, T. F., Osman, M. G. "Probabilistic power quality indices for electric grids with increased penetration level of wind power generation", *International Journal of Electrical Power & Energy Systems*, 77, pp. 50–58, 2016. <https://doi.org/10.1016/j.ijepes.2015.09.026>
- [11] Prakash Mahela, O., Gafoor Shaik, A. "Topological aspects of power quality improvement techniques: A comprehensive overview", *Renewable and Sustainable Energy Reviews*, 58, pp. 1129–1142, 2016. <https://doi.org/10.1016/j.rser.2015.12.251>
- [12] Pedapenki, K. K., Gupta, S. P., Pathak, M. K. "Shunt active power filter with artificial intelligent controllers", In: *2015 International Conference on Control, Instrumentation, Communication and Computational Technologies (ICCICCT)*, Kumaracoil, India, 2015, pp. 74–77. ISBN 978-1-4673-9825-1 <https://doi.org/10.1109/ICCICCT.2015.7475252>
- [13] Al-Dwa, A. A. M., Chebabhi, A., Defdaf, M., Guessabi, A. "New Modeling and Improved Current Control Strategy to Eliminate the Impact of Synchronization Method and Parks Transformation for Grid-connected Four-leg PWM Inverter", *Periodica Polytechnica Electrical Engineering and Computer Science*, 67(2), pp. 204–215, 2023. <https://doi.org/10.3311/PPee.20517>

- [14] Pedapenki, K. K., Gupta, S. P., Pathak, M. K. "Shunt active power filter with MATLAB and dSPACE 1104 verification", *International Journal of Applied Engineering Research*, 11(6), pp. 4085–4090, 2016.
- [15] Hooshmand, R. A., Torabian Esfahani, M. "Adaptive Filter Design Based on the LMS Algorithm for Delay Elimination in TCR/FC Compensators", *ISA Transactions*, 50(2), pp. 142–149, 2011. <https://doi.org/10.1016/j.isatra.2010.12.002>
- [16] Murugesan, K., Muthu, R., Vijayenthiran, S., Mervin, J. B. "Prototype Hardware Realization of the DSTATCOM for Reactive Power Compensation", *International Journal of Electrical Power & Energy Systems*, 65, pp. 169–178, 2015. <https://doi.org/10.1016/j.ijepes.2014.09.032>
- [17] Hingorani, N. G., Gyugyi, L. "Understanding FACTS: Concepts and technology of flexible AC transmission systems", Wiley-IEEE Press, 1999. ISBN 0-7803-3455-8
- [18] Saad, S., Zellouma, L. "Fuzzy logic controller for three-level shunt active filter compensating harmonics and reactive power", *Electric Power Systems Research*, 79(10), pp. 1337–1341, 2009. <https://doi.org/10.1016/j.epsr.2009.04.003>
- [19] Maharjan, L., Inoue, S., Akagi, H. "A Transformerless Energy Storage System Based on a Cascade Multilevel PWM Converter with Star Configuration", *IEEE Transactions on Industry Applications*, 44(5), pp. 1621–1630, 2008. <https://doi.org/10.1109/TIA.2008.2002180>
- [20] Xiao, P., Venayagamoorthy, G. K., Corzine, K. A. "Seven-level shunt active filter for high-power drive systems", *IEEE Transactions on Power Electronics*, 24(1), pp. 6–13, 2009. <https://doi.org/10.1109/TPEL.2008.2005897>
- [21] Salimon, S. A., Lawal, Q. O., Adebisi, O. W., Okelola, M. O. "Cost-Benefit of Optimal Allocation of DSTATCOM in Distribution Networks Using Ant-Lion Optimization Algorithm", *Periodica Polytechnica Electrical Engineering and Computer Science*, 66(4), pp. 350–360, 2022. <https://doi.org/10.3311/PPee.20549>
- [22] Shyu, K.-K., Yang, M.-J., Chen, Y.-M., Lin, Y.-F. "Model reference adaptive control design for a shunt active-power-filter system", *IEEE Transactions on Industrial Electronics*, 55(1), pp. 97–106, 2008. <https://doi.org/10.1109/TIE.2007.906131>
- [23] Chawda, G. S., Shaik, A. G. "Smooth grid synchronization in weak AC grid with high wind energy penetration using distribution static compensator", In: 2019 2nd International Conference on Smart Grid and Renewable Energy (SGRE), Doha, Qatar, 2019, pp. 1–6. ISBN 978-1-7281-2961-7 <https://doi.org/10.1109/SGRE46976.2019.9020671>
- [24] Singh, B., Solanki, J. "An implementation of an adaptive control algorithm for a three-phase shunt active filter", *IEEE Transactions on Industrial Electronics*, 56(8), pp. 2811–2820, 2009. <https://doi.org/10.1109/TIE.2009.2014367>
- [25] Pedapenki, K. K., Swathi, G. "Analysis of shunt active power filter with unit voltage template method", In: 2017 International Conference on Computation of Power, Energy Information and Communication (ICCPEIC), Melmaruvathur, India, 2017, pp. 749–753. ISBN 978-1-5090-4325-5 <https://doi.org/10.1109/ICCPEIC.2017.8290463>
- [26] Pedapenki, K. K., Gupta, S. P., Pathak, M. K. "Fuzzy membership functions based active filter for power quality improvement", In: 2015 International Conference on Control, Instrumentation, Communication and Computational Technologies (ICCICCT), Kumaracoil, India, 2015, pp. 231–235. ISBN 978-1-4673-9825-1 <https://doi.org/10.1109/ICCICCT.2015.7475281>
- [27] Singh, B., Dube, S. K., Arya, S. R. "An Improved Control Algorithm of DSTATCOM for Power Quality Improvement", *International Journal of Electrical Power & Energy Systems*, 64, pp. 493–504, 2015. <https://doi.org/10.1016/j.ijepes.2014.07.055>
- [28] Ajami, A., Taheri, N. "A Hybrid Fuzzy/LQR Based Oscillation Damping Controller Using 3-level STATCOM", *International Journal of Computer Electronics Engineering*, 3(2), pp. 184–189, 2011. <https://doi.org/10.7763/IJCEE.2011.V3.312>
- [29] Mariun, N., Hizam, H., Izzri, A. W. N., Aizam, S. "Design of the Pole Placement Controller for D-STATCOM in Mitigating Three Phase Fault", In: 2005 IEEE Power Engineering Society Inaugural Conference and Exposition in Africa, Durban, South Africa, 2005, pp. 349–355. ISBN 0-7803-9326-0 <https://doi.org/10.1109/PESAfr.2005.1611844>
- [30] Coteli, R., Dandil, B., Ata, F. "Fuzzy-PI current controlled D-STATCOM", *Gazi University Journal of Science*, 24(1), pp. 91–99, 2011.
- [31] Venayagamoorthy, G. K., Harley, R. G. "Computational intelligence techniques for control of FACTS device", In: Chow, J. H., Wu, F. F., Momoh, J. (eds.) *Applied Mathematics for Restructured Electric Power Systems*, 2005, pp. 201–237. ISBN 978-0-387-23470-0 https://doi.org/10.1007/0-387-23471-3_10
- [32] Pedapenki, K. K., Gupta, S. P., Pathak, M. K. "Comparison of Fuzzy Logic and Neuro Fuzzy Controller for Shunt Active Power Filter", In: 2015 International Conference on Computational Intelligence and Communication Networks (CICN), Jabalpur, India, 2015, pp. 1247–1250. ISBN 978-1-5090-0077-7 <https://doi.org/10.1109/CICN.2015.240>
- [33] Karnik, N. N., Mendel, J. M., Liang, Q. "Type-2 fuzzy logic systems", *IEEE Transactions on Fuzzy Systems*, 7(6), pp. 643–658, 1999. <https://doi.org/10.1109/91.811231>
- [34] Singh, B., Adya, A., Mittal, A. P., Gupta, J. R. P. "Modelling and control of DSTATCOM for three-phase, four-wire distribution systems", In: Fortieth IAS Annual Meeting. Conference Record of the 2005 Industry Applications Conference, 2005., vol. 4, Hong Kong, China, 2005, pp. 2428–2434. ISBN 0-7803-9208-6 <https://doi.org/10.1109/IAS.2005.1518801>
- [35] Benzerafa, F., Tlemçani, A., Sebaa, K. "Type-1 and type-2 fuzzy logic controller based multilevel DSTATCOM using SVM", *Studies in Informatics and Control*, 25(1), pp. 87–98, 2016. <https://doi.org/10.24846/v25i1y201610>
- [36] Singh, B. N., Venkata Srinivas, K., Chandra, A., Al Haddad, K. "A new configuration of 12-pulse VSCs based STATCOM with constant DC link voltage", presented at 4th International Conference on Computer Applications in Electrical Engineering Recent Advances (CERA), IIT Roorkee, India, Feb. 19–21, 2010. [online] Available at: <https://espace2.etsmtl.ca/id/eprint/353/> [Accessed: 04 March 2023]

- [37] Chatterjee, S. A., Joshi, K. D. "A Comparison of Conventional, Direct-Output-Voltage and Fuzzy-PI Control Strategies for D-STATCOM", In: 2010 Modern Electric Power Systems, Wroclaw, Poland, 2010, pp. 1–6. ISBN 978-83-921315-8-8
- [38] Kumar, N. M. G., Raju, P. S., Venkatesh, P. "Control of DC Capacitor Voltage in a DSTATCOM using Fuzzy Logic Controller", International Journal of Advances in Engineering & Technology, 4(1), pp. 679–691, 2012.
- [39] Abdur Rahim, A. H. M., Al-Baiyat, S. A., Kandlawala, M. F. "A Fuzzy STATCOM Control for power System Damping Enhancement", In: 2nd IEEE GCC Conference, Manama, Bahrain, 2004, pp. 463–467.
- [40] Sivakumar, A., Thiyagarajan, M., Kanagarathinam, K. "Mitigation of supply current harmonics in fuzzy-logic based 3-phase induction motor", International Journal of Power Electronics and Drive Systems (IJPEDS), 14(1), pp. 266–274, 2023.
<https://doi.org/10.11591/ijpeds.v14.i1.pp266-274>
- [41] Pedapenki, K. K., Gupta, S. P., Pathak, M. K. "Two controllers for shunt active power filter based on fuzzy logic", In: 2015 IEEE International Conference on Research in Computational Intelligence and Communication Networks (ICRCICN), Kolkata, India, 2015, pp. 141–144. ISBN 978-1-4673-6735-6
<https://doi.org/10.1109/ICRCICN.2015.7434225>
- [42] Suresh, D., Kumar, T. J., Singh, S. P. "Three-level active neutral point clamped DSTATCOM with Interval Type-2 fuzzy logic controller", In: 2020 International Conference on Computer Communication and Informatics (ICCCI), Coimbatore, India, 2020, pp. 1–5. ISBN 978-1-7281-4515-0
<https://doi.org/10.1109/ICCCI48352.2020.9104204>
- [43] Suresh, D., Venkateswarlu, K., Singh, S. P. "T2FLC based CHBMLI DSTATCOM for power quality Improvement", In: 2018 International Conference on Computer Communication and Informatics (ICCCI), Coimbatore, India, 2018, pp. 1–6. ISBN 978-1-5386-2239-1
<https://doi.org/10.1109/ICCCI.2018.8441224>
- [44] Pandu, S. B., Sundarabalan, C. K., Srinath, N. S., Krishnan, T. S., Priya, G. S., Balasundar, C., Sharma, J., Soundarya, G., Siano, P., Alhelou, H. H. "Power Quality Enhancement in Sensitive Local Distribution Grid Using Interval Type-II Fuzzy Logic Controlled DSTATCOM", IEEE Access, 9, pp. 59888–59899, 2021.
<https://doi.org/10.1109/ACCESS.2021.3072865>
- [45] Kadri, A., Makhloufi, S. "Interval Type2 Fuzzy Logic Based STATCOM Controller for Stabilizing a Mixed Electrical Network System", Periodica Polytechnica Electrical Engineering and Computer Science, 66(4), pp. 391–405, 2022.
<https://doi.org/10.3311/PPee.19822>
- [46] Drak Alsebai, M., Narayanan, K., Pedapenki, K. K. "Adaptive Interval Type II Fuzzy Logic Controller with Interface Inductor Bank Pulse Generator Based Three-Phase Four-Wire DSTATCOM Device for Power Quality Improvement", Periodica Polytechnica Electrical Engineering and Computer Science, 67(2), pp. 113–135, 2023.
<https://doi.org/10.3311/PPee.20890>
- [47] Jayachandran, J., Murali Sachithanandam, R. "Neural Network-Based Control Algorithm for DSTATCOM Under Nonideal Source Voltage and Varying Load Conditions", Canadian Journal of Electrical and Computer Engineering, 38(4), pp. 307–317, 2015.
<https://doi.org/10.1109/CJECE.2015.2464109>
- [48] Arya, S. R., Singh, B. "Neural network based conductance estimation control algorithm for shunt compensation", IEEE Transactions on Industrial Informatics, 10(1), pp. 569–577, 2014.
<https://doi.org/10.1109/TII.2013.2264290>
- [49] Kadem, M., Semmah, A., Wira, P., Slimane, A. "Artificial Neural Network Active Power Filter with Immunity in Distributed Generation", Periodica Polytechnica Mechanical Engineering, 64(2), pp. 109–119, 2020.
<https://doi.org/10.3311/PPme.12775>
- [50] Alsebai, M. D., Kamala, N. "Source Current-Voltage Loop Based Instantaneous Reactive Power Theory Control Algorithm Based DSTATCOM for Power Quality Improvement", University Politehnica of Bucharest Scientific Bulletin, Series C, 84(2), pp. 337–352, 2022.
- [51] Taskin, A., Kumbasar, T. "An Open-Source Matlab/Simulink Toolbox for Interval Type-2 Fuzzy Logic Systems", In: 2015 IEEE Symposium Series on Computational Intelligence, Cape Town, South Africa, 2015, pp. 1561–1568. ISBN 978-1-4799-7560-0
<https://doi.org/10.1109/SSCI.2015.220>